



1 **Where to GreenDrill? Site selection for cosmogenic nuclide exposure dating of**  
2 **the bed of the Greenland Ice Sheet**

3

4 Jason P. Briner<sup>1\*</sup>, Caleb K. Walcott<sup>1</sup>, Joerg M. Schaefer<sup>2</sup>, Nicolás E. Young<sup>2</sup>, Joseph A.  
5 MacGregor<sup>3</sup>, Kristin Poinar<sup>1</sup>, Benjamin A. Keisling<sup>2</sup>, Sridhar Anandakrishnan<sup>4</sup>, Mary R. Albert<sup>5</sup>,  
6 Tanner Kuhl<sup>6</sup> and Grant Boeckmann<sup>6</sup>

7

8 *1 Department of Geology, University at Buffalo, Buffalo, NY, 14260 USA*

9 *2 Lamont-Doherty Earth Observatory, Columbia University, Palisades, NY, USA*

10 *3 Cryospheric Sciences Laboratory, NASA Goddard Space Flight Center, Greenbelt, Maryland,*  
11 *USA*

12 *4 Department of Geosciences, Penn State University, University Park, PA 16802, USA*

13 *5 U.S. Ice Drilling Program, Thayer School of Engineering, Dartmouth College, Hanover, NH, USA*  
14 *Ice Drilling Program*

15 *6 U.S. Ice Drilling Program, University of Wisconsin-Madison, Madison, WI, USA*

16

17 *\*Corresponding author, jbriner@buffalo.edu*

18

19

20

21

22

23

24

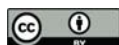
25

26

27

28

29



30 **1. Abstract**

31 Direct observations of the size of the Greenland Ice Sheet during Quaternary interglaciations  
32 are sparse yet valuable for testing numerical models of ice sheet history and sea level  
33 contribution. Recent measurements of cosmogenic nuclides in bedrock from beneath the  
34 Greenland Ice Sheet collected during past deep drilling campaigns reveal that the ice sheet was  
35 significantly smaller, and perhaps largely absent, sometime during the past 1.1 million years.  
36 These discoveries from decades-old basal samples motivate new, targeted sampling for  
37 cosmogenic nuclide analysis beneath the ice sheet. Current drills available for retrieving bed  
38 material from the US Ice Drilling Program require <700 m ice thickness and a frozen bed, while  
39 quartz-bearing bedrock lithologies are required for measuring a large suite of cosmogenic  
40 nuclides. We find that these and other requirements yield only ~3.4% of the Greenland Ice  
41 Sheet bed as a suitable drilling target using presently available technology. Additional factors  
42 related to scientific questions of interest are which areas of the present ice sheet are the most  
43 sensitive to warming, where a retreating ice sheet would expose bare ground rather than leave  
44 a remnant ice cap, and which areas are most likely to remain frozen bedded throughout glacial  
45 cycles and thus best preserve cosmogenic nuclides? Here we identify locations beneath the  
46 Greenland Ice Sheet that are best suited for potential future drilling and analysis. These include  
47 sites bordering Inglefield Land in northwestern Greenland, near Victoria Fjord and Mylius-  
48 Erichsen Land in northern Greenland, and inland from the alpine topography along the ice  
49 margin in eastern and northeastern Greenland.

50

51 **2. Introduction**

52 Recent observations reveal significant ice loss in Greenland and Antarctica, with the  
53 Greenland Ice Sheet (GrIS) presently contributing more to sea level rise than the Antarctic Ice  
54 Sheet (AIS) (Shepherd et al., 2018; Shepherd et al., 2020). The higher potential for portions of  
55 the AIS to collapse due to marine ice-sheet instability, however, leaves estimates of future sea  
56 level rise highly uncertain (Scambos et al., 2017; DeConto et al., 2021; Edwards et al., 2021).  
57 Non-linearities in ice sheet response to climate change also apply to the GrIS, which has been  
58 simulated to disappear in as little as one millennium (Aschwanden et al., 2019). Estimated rates



59 of GrIS loss this century under the current trajectory of greenhouse-gas emissions (Goelzer et  
60 al., 2020; Edwards et al., 2021) have been shown to exceed those under natural variability over  
61 the past 12,000 years (Briner et al., 2020).

62 Although present rates of ice sheet loss are exceptional and concerning, there are few  
63 direct constraints on GrIS and AIS response to similar warmth during past interglaciations of the  
64 Quaternary (e.g., deVernal and Hillaire-Marcel, 2008; Schaefer et al., 2016). Thus, knowledge of  
65 ice sheet response under past climates that are comparable to the climate of our near future  
66 remains limited. Proxy data from geological archives, such as sedimentological characteristics in  
67 adjacent seas, have been used to evaluate ice sheet history. For example, a growing body of  
68 evidence from offshore Greenland documents overall ice sheet growth and its subsequent  
69 oscillatory configurations throughout the Pliocene and Quaternary (e.g., Bierman et al., 2016,  
70 Knutz et al., 2019). Paleoceanographic studies have made valuable inferences of climate  
71 conditions (e.g., de Vernal and Hillaire-Marcel, 2008; Cluett and Thomas, 2021) and ice sheet  
72 configuration (e.g., Reyes et al., 2014; Hatfield et al., 2016) during brief interglacials, but  
73 generating direct knowledge of past GrIS response to interglacial warmth has proven difficult  
74 with these approaches. Farfield sea level reconstructions help to constrain GrIS response during  
75 past interglaciations (e.g., Dyer et al., 2021), yet still benefit from direct observations from  
76 individual ice sheets. Ice sheet modeling has simulated a variety of ice sheet volumes and  
77 configurations during past interglaciations (e.g., Goelzer et al., 2016; Robinson et al., 2017;  
78 Plach et al., 2018; Sommers et al., 2021), indicating more geologic measurements of ice-sheet  
79 extent are needed to evaluate these results.

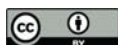
80 The age of ice in basal ice core sections has been used to constrain the GrIS  
81 configuration during marine isotope stage (MIS) 5e (129-116 ka) and thus validate numerical  
82 simulations of ice size and configuration during the last interglacial (Otto-Bleisner et al., 2006;  
83 Plach et al., 2018; Domingo et al., 2020). However, there is some uncertainty about the role  
84 that ice advection plays in bringing aged ice over a previously ice-free location. For example,  
85 Yau et al. (2016a) found that the best fitting models for matching their elevation and  
86 temperature reconstructions for NEEM and GISP2 did not have ice at NEEM during the MIS 5e,  
87 implying that the MIS 5e ice recovered at NEEM today not only flowed laterally but re-



88 advanced over a deglaciated landscape. This phenomenon can be observed directly at the  
89 modern ice-sheet margin today, where Pleistocene-age ice outcrops at the margin in western  
90 Greenland (e.g., Reeh et al. 2002; MacGregor et al. 2020) where there was no ice as recently as  
91 the middle Holocene (Briner et al., 2010). Thus, it is critical to obtain independent information  
92 about sub-ice bedrock exposure age because apparently the age/stratigraphy of the overlying  
93 ice does not necessarily provide a continuous constraint on ice-cover history.

94 Fortunately, a new frontier of science is emerging, aimed at generating direct  
95 constraints on former ice sheet size using information collected from the ice sheet bed.  
96 Schaefer et al. (2016) measured cosmogenic  $^{10}\text{Be}$  and  $^{26}\text{Al}$  in bedrock obtained below the GISP2  
97 ice core (Figure 1), equipped with updated procedures and vastly improved analytic sensitivity  
98 relative to an earlier attempt (Nishiizumi et al., 1996). Their measurements require the GrIS to  
99 have been absent at the GISP2 locality for 280 kyr of the past 1.4 Myr. Although alternative  
100 histories are possible, the results point to significant ice loss in Greenland within the  
101 Quaternary, and likely within the last 1.1 Myr. More recently, Christ et al. (2021) measured  
102 cosmogenic  $^{10}\text{Be}$  and  $^{26}\text{Al}$  in re-discovered sub-ice sediments in the Camp Century core  
103 collected in the 1960s (Figure 1). They interpret their results to indicate that the landscape  
104 below Camp Century became ice free at least once in the last 1.0 Myr. While one might expect  
105 the GrIS flank site of Camp Century to become ice free during some interglacial periods (model  
106 simulations commonly show this; Plach et al., 2018; Sommers et al., 2021), the findings from  
107 beneath the summit of the GrIS were more unexpected because model simulations rarely show  
108 ice-free conditions there (Briner et al., 2017). Additionally, new approaches have been  
109 developed to solve for long-term ice sheet occupation and subglacial erosion histories from  
110 vertical profiles of cosmogenic nuclides measured in multiple meters of rock core (Balter-  
111 Kennedy et al., 2021). Performing such analyses on new multi-meter-long bedrock cores from  
112 beneath the GrIS will be key for deciphering GrIS history.

113 Cosmogenic-nuclide measurements from sub-ice bed material in Greenland already  
114 have been shown to place direct constraints on past ice sheet history, despite the study of only  
115 two cosmogenic isotopes ( $^{10}\text{Be}$  and  $^{26}\text{Al}$ ) in these samples thus far. Additionally, the recent  
116 results from the sub-GrIS environment, although derived using legacy material from sites not



117 targeted for cosmogenic-nuclide measurements, have demonstrated the power of this  
118 approach. While drilling technology that allows quick access (i.e., in a single field season) to the  
119 bed below ice sheet summits is being developed for application in Antarctica (Goodge and  
120 Severinghaus, 2016; Goodge et al., 2021), there is no such drill – or plans for one – to operate in  
121 Greenland. However, there are drills designed to quickly access the bed in locations where ice  
122 thickness is less than ~700 m (Spector et al., 2017, 2018). The goal of this study is to survey  
123 Greenland to identify sites that are potentially suitable for sub-ice cosmogenic-nuclide  
124 measurements using two suitable drills in the US Ice Drilling Program’s inventory: the Agile Sub-

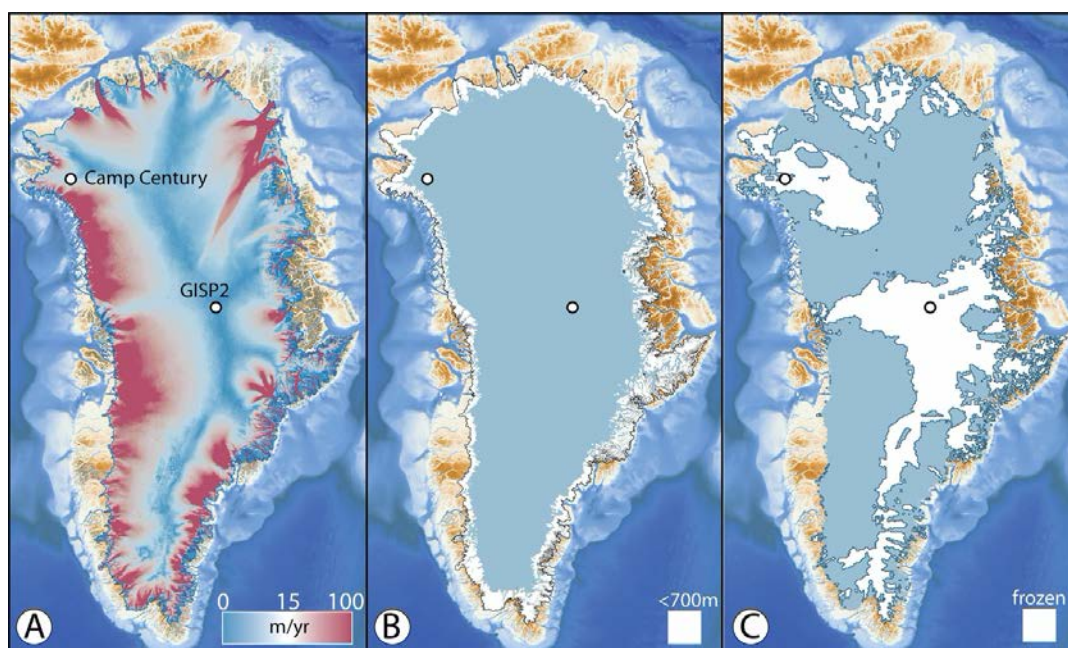
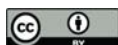


**Figure 1.** (A) Horizontal surface velocities of the Greenland Sheet; the slowest flowing-areas define the summit ridge and ice divides; velocity from Greenland Ice Sheet velocity map from Sentinel-1, winter campaign 2019/2020 [version 1.3]; QGreenland v2.0. (B) The pattern of <700 m ice thickness (white) shown around perimeter of the ice sheet, which covers 15.2% of the ice-sheet footprint. (C) Where the basal thermal state is likely frozen bedded (white), which covers 37.4% of the ice-sheet footprint (from MacGregor et al., 2022). Basemap topography and bathymetry from Morlighem et al. (2017).

125 Ice Geological (ASIG; Kuhl et al., 2021) drill and the Winke Drill (Boeckmann et al., 2021). Both  
126 of these drills can operate in Greenland. Considering drill specifications, scientific and safety  
127 criteria, we identify multiple suitable sites near the GrIS margin across northern and eastern  
128 Greenland. These sites represent candidate targets for the GreenDrill project supported by the  
129 U.S. National Science Foundation.



130

### 131 **3 Considerations for drilling**

132           The drills currently available from the US Ice Drilling Program that are designed to drill  
133 rock cores beneath tens to hundreds of meters of glacial ice require the bed beneath the ice to  
134 be frozen to its bed. Additional specifications for scientific projects focused on sub-ice samples  
135 obtained via drilling, such as bedrock lithology and site accessibility, further limit suitable areas.  
136 The bedrock lithology of Greenland is varied and is only exposed around the island's perimeter  
137 and directly observable in only one hand-sample from the base of the GISP2 ice core site. With  
138 only six locations across the GrIS interior where boreholes have reached the bed, there are also  
139 limited direct observations of the ice sheet's basal thermal state. Below, we compile this and  
140 other necessary information for identifying potential sites for retrieval of rock cores beneath  
141 the GrIS.

142

#### 143 **3.1 Drills**

144           We first briefly outline the technical requirements of the two presently available US Ice  
145 Drilling Program drills designed to drill through ice and into the underlying bedrock: ASIG and  
146 Winkie (Albert et al., 2020). The ASIG Drill is currently designed to drill access holes through ice  
147 <700 m thick and collect bedrock cores several meters long. It requires frozen basal conditions  
148 to ensure that drilling fluid is maintained in the entire borehole across the ice–bed interface.  
149 The ASIG drill was successfully used in West Antarctica near the Pirrit Hills in 2016–2017, where  
150 it drilled through approximately 150 m of ice and collected 8 m of 39-mm-diameter rock core of  
151 excellent quality (Kuhl et al., 2021). Nearly 5 m of ice core was also collected near the ice-  
152 bedrock transition, however, the core quality was poor. The Winkie Drill is capable of drilling  
153 120 m of ice and rock (e.g., it can retrieve a 10 m rock core from beneath 110 m of ice); it also  
154 has the requirement of a frozen bed. Given these restrictions, the Winkie Drill is mostly  
155 restricted to frozen-bedded environments very near the GrIS margin, and the ASIG Drill is  
156 suitable to drill in similar environments slightly farther inland.

157

#### 158 **3.1 Ice thickness**



159           The large-scale thickness of the GrIS is relatively well known, stemming from several  
160 decades of radar data collection by NASA and European institutions (e.g., Li et al, 2012).  
161 Morlighem et al. (2017) combined airborne radar-sounding-derived ice thickness data with  
162 comprehensive, high-resolution ice motion measurements derived from satellite  
163 interferometric synthetic-aperture radar. This combination of datasets allowed Morlighem et  
164 al. (2017) to employ a mass conservation algorithm (Morlighem et al., 2011; McNabb et al  
165 2012) to calculate ice thickness around the periphery of the GrIS. They produced a map of bed  
166 topography by subtracting ice thickness from a digital elevation model of the ice surface. Mass  
167 conservation works best in areas of fast flow, where uncertainty in flow direction is small and  
168 the glaciers mostly flow due to basal motion (Morlighem et al., 2011). In the interior, where  
169 deformation is likely a more dominant component of ice flow and uncertainty in flow direction  
170 is greater, they employed ordinary kriging to interpolate ice thickness measurements. We use  
171 BedMachine v3 (Morlighem et al., 2017) and ArcGIS to deduce that 15.2% of the GrIS is <700 m  
172 in thickness (Figure 1B).

173

### 174 ***3.2 The basal thermal state of the GrIS***

175           Due to the limited number of boreholes that have reached the GrIS bed, its basal  
176 thermal state must presently be estimated from a synthesis of multiple methods. MacGregor et  
177 al. (2016, 2022) combined thermomechanical ice-flow models and inferences from airborne  
178 and satellite remote sensing to constrain where the bed is likely thawed, where it is likely  
179 frozen and where it remains too uncertain to specify, at a spatial resolution of 5 km. The latest  
180 version of this synthesis of the GrIS likely basal thermal state (MacGregor et al., 2022) is shown  
181 in Figure 1C. The map suggests frozen-bedded conditions across 37.4% of the ice sheet, mostly  
182 beneath ice divides and parts of North Greenland (Figure 2). The ice margin and near-ice-  
183 margin areas throughout most of Greenland are largely believed to be thawed, except for a few  
184 locations across North and East Greenland where frozen-bedded conditions are ubiquitous –  
185 even near the ice margin. However, there are many areas where the basal thermal state is

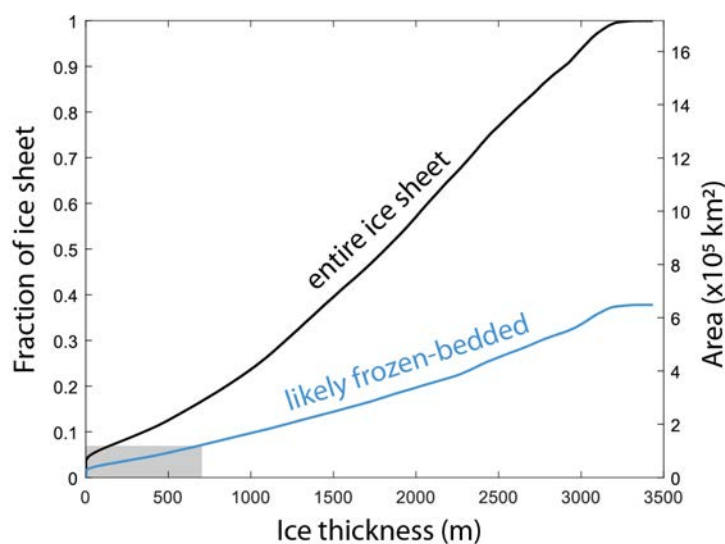
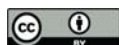
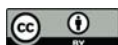


**Figure 2.** Greenland Ice Sheet thickness versus area. Plot shows that only about one-third of the ice sheet by area is likely frozen-bedded, and thus available for subglacial access. The current limit of drills of operating under 700 m ice thickness further reduces available portion of the ice-sheet bed for access (gray area). Note that increasing a drill's depth capability increases the area of the bed available for drilling; the ability to drill into wet-based sections of the ice sheet would significantly increase the area available for drilling.

186 mapped as uncertain (i.e., areas that are inconclusive in terms of their likelihood to be either  
187 warm-or frozen-bedded), and many of these areas also extend to the ice margin in portions of  
188 North and East Greenland. Jordan et al. (2018) used radar returns to identify locations of  
189 probable water at the bed. Although the method could not be applied throughout Greenland  
190 due to limitations in radar extent and quality, their fine-resolution dataset was included by  
191 MacGregor et al. (2022). Bedrock weathering textures and landforms observed in landscapes  
192 occupied by Pleistocene ice sheets reveal sharp transitions between warm- and frozen-bedded  
193 conditions in the past, particularly in areas of high topographic relief (e.g., Sugden, 1978; Briner  
194 et al., 2006). Thus, there could be localized patches of frozen-bedded conditions across many  
195 areas around the GrIS perimeter that are too small in scale to be suitably represented using the  
196 methods of Jordan et al. (2018) and MacGregor et al. (2022). Combining likely frozen basal  
197 conditions with ice thicknesses <700 m results in 6.8% of the bed available for drilling (Figures 2  
198 and 3A).





199 Finally, prior to drilling, the selected sites should be assessed with geophysical methods  
200 to further estimate the thermal state of the bed. Existing radar profiles combined with new  
201 radar and seismic measurements can reduce the uncertainty about the condition of the bed.  
202 Seismic methods can more confidently measure whether a significant water volume is present  
203 at the bed, either pooled or within sediment pores (e.g., Kulesa et al., 2017). The reflectivity of  
204 water or water-laden sediments is significantly different than for frozen sediments. Note that a  
205 thin layer of water over crystalline bedrock would be difficult to distinguish from frozen ice over  
206 bedrock.  
207

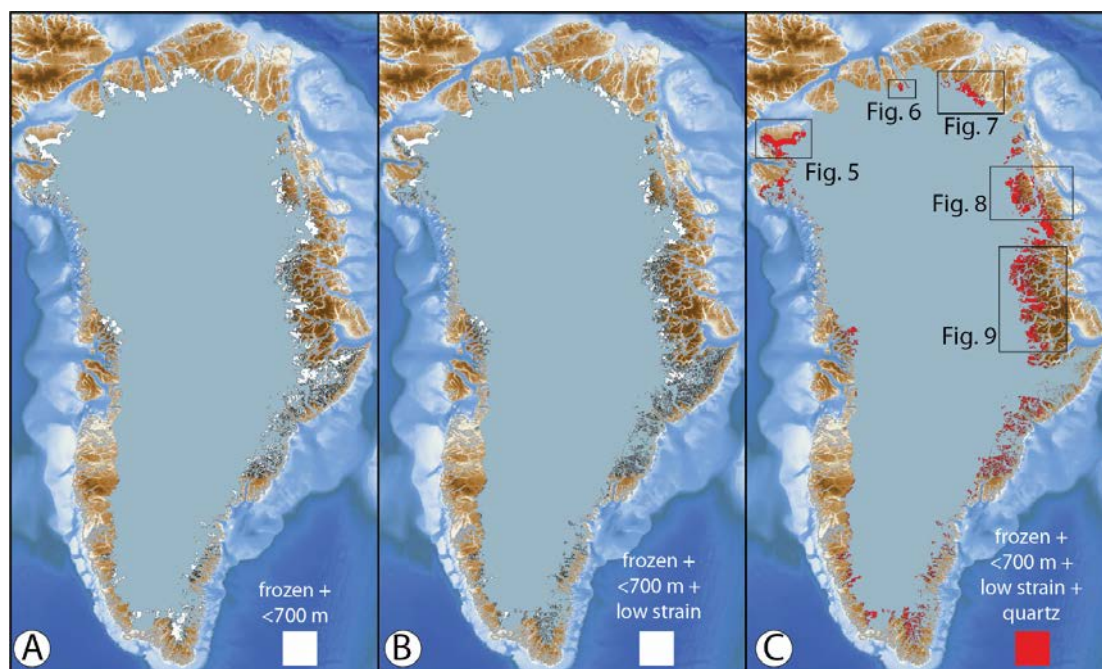


**Figure 3.** (A) Portion of the Greenland Ice Sheet bed (6.8%) that are both likely frozen and beneath <700 m of ice. (B) Same as in A but which has a low likelihood of surface crevasses (4.8%). (C) Same as in B but with likely quartz-bearing lithologies (3.4%). Basemap topography and bathymetry from Morlighem et al. (2017).

### 208 **3.3 Surface features, safety and site accessibility**

209 Because available drills require <700 m ice thickness, the viable areas of interest are  
210 mostly restricted to near the ice margin (Figure 1B). These areas generally have high surface  
211 velocity (>50 m/yr) and spatial variability in surface velocity as ice flow becomes increasingly  
212 influenced by underlying topography (Figure 1A). Consequently, these areas have high strain



213 rates and can be heavily crevassed, making them some of the most dangerous locations on the  
214 GrIS to work. However, not all ice-marginal areas exhibit high velocity and high strain rates, so  
215 some areas are relatively crevasse free. Surface strain rates derived from GrIS surface velocity  
216 (Figure 1A) can guide site selection for low likelihood of crevassing. In this way, one can address  
217 the criterion of being most likely to be safe for air support and/or access via traverse vehicles.  
218 We use a strain-rate field from Poinar and Andrews (2021) and a threshold value of 0.005/year,  
219 above which crevasses are likely to form (Joughin et al., 2013). This analysis further reduces the  
220 area of the GrIS suitable for drilling from 6.8% to 4.8% (Figure 3B).

221

### 222 **3.4 Cosmogenic nuclides and subglacial geology**

223 An entire family of cosmogenic nuclides are routinely measured in Earth materials. Most  
224 research to date in Earth science, however, has used cosmogenic nuclides produced in quartz:  
225  $^{26}\text{Al}$ ,  $^{14}\text{C}$  and  $^{10}\text{Be}$  (Granger et al., 2013; Briner et al., 2014; Balco, 2020). While there are  
226 cosmogenic nuclides that can be used in mafic lithologies (e.g.,  $^{36}\text{Cl}$ ,  $^3\text{He}$ ) and carbonates (e.g.,  
227  $^{36}\text{Cl}$ ), the advantage of quartz is that the trio of  $^{26}\text{Al}$ ,  $^{14}\text{C}$  and  $^{10}\text{Be}$  can all be measured together  
228 (e.g., Young et al., 2021). These three nuclides have widely spaced half lives, providing a  
229 powerful exposure-burial chronometer well suited for providing direct constraints on ice sheet  
230 history. Additionally,  $^{36}\text{Cl}$  can also be measured in feldspars, and thus targeting felsic-crystalline  
231 lithologies potentially offers a fourth cosmogenic nuclide with a unique half-life for analysis.

232 A bedrock substrate has advantages over sediment deposits, although cosmogenic  
233 nuclide measurements from both are informative. Sediments beneath ice sheets are more  
234 easily eroded, deformed, entrained and transported and re-deposited than bedrock. Thus,  
235 cosmogenic nuclide concentrations from the sediment grains themselves, which have a  
236 transport and deposition history, can be more complicated to interpret than those in bedrock.  
237 For targeted sub-GrIS cosmogenic nuclide campaigns, the highest priority sites are those where  
238 non-erosive ice rests directly on quartz-bearing bedrock.

239 Because 81% of Greenland's land area lies beneath the ice, bedrock geology has only  
240 been mapped across 19% of Greenland. There is a large degree of uncertainty about the  
241 lithology below the ice sheet. Dawes (2009) inferred the sub-GrIS geology based on information



242 from six methods: Drill sites, nunataks, coast-to-coast correlation, glacial erratics, detrital  
243 provenance studies and geophysics. For our purposes, we provide a highly abbreviated  
244 overview of this geology with particular attention paid to quartz-bearing lithologies in areas  
245 likely to coincide with frozen-bedded conditions. We use the geologic map of Greenland,  
246 available online at <https://www.greenmin.gl/> (Pedersen et al., 2013; Henriksen et al., 2009).  
247 Generally, Greenland mostly consists of Precambrian shield rocks (both Archean and  
248 Proterozoic; largely quartz-bearing) in its south, west and center. North Greenland consists of  
249 Paleozoic basins containing mostly non-quartz-bearing lithologies. East and Northeast  
250 Greenland comprise the Caladonian fold belt and a complex pattern of Proterozoic rocks of  
251 mixed lithology, although these are thought to be mainly limited to the island's periphery.  
252 Portions of the central east and central west coasts of Greenland contain Paleogene volcanic  
253 lithologies that may connect beneath the central GrIS. North Greenland generally encompasses  
254 the highest proportion of the margin and near-margin areas thought to be frozen-bedded;  
255 however, carbonate and other non-quartz-bearing lithologies dominate these areas. We use  
256 the geologic map of Greenland to categorize bedrock lithology into quartz-bearing and non-  
257 quartz-bearing units (Figure 4). We remove the ice-marginal areas adjacent to carbonate and  
258 volcanic lithologies from consideration, which reduces the target area from 4.8% to 3.4% of the  
259 GrIS (Figure 3C).

260 In addition to lithology considerations, one may prefer to generate depth profiles of  
261 cosmogenic nuclides in bedrock as opposed to in sediment, as mentioned above. Site selection  
262 is aided by airborne radar sounding data obtained by NASA Operation Ice Bridge. Existing  
263 surveys of the ice sheet bed are inadequate for identifying every low topographic swale that  
264 could potentially be sediment filled, particularly between radar flight lines. However, by  
265 avoiding valleys and low areas and instead opting for mountain summits or plateaus, we can  
266 increase the likelihood of drilling into bedrock with thin or no sediment cover. Although not  
267 always the case, in most areas on Greenland that are ice free today, bare bedrock surfaces  
268 generally exist in higher proportion on hilltops and uplands, as opposed to low-lying areas and  
269 valley bottoms. Thus, choosing sites along radar flight lines ensures the most reliable  
270 knowledge of bed topography and ice thickness at a candidate drill site.



271

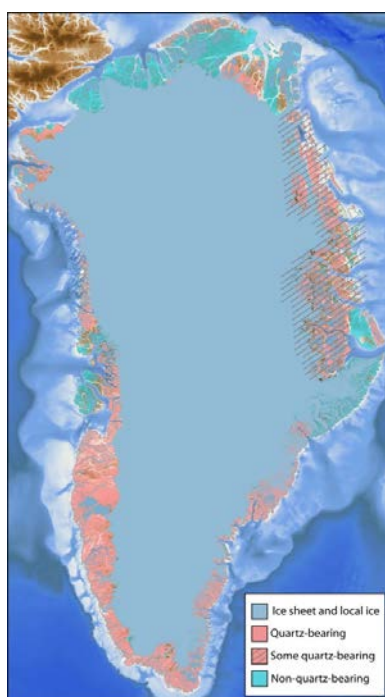
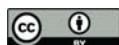


**Figure 4.** Simplified bedrock geology map of Greenland, showing lithology sub-divided into probably quartz-bearing rocks, some quartz bearing lithologies and probably non-quartz-bearing rocks. From <https://www.greenmin.gl/>. Basemap topography and bathymetry from Morlighem et al. (2017).

### 272 **3.5 Strategizing drill site selection related to scientific motivation**

273 Having applied above the drilling and geologic requirements for site selection, we next  
274 consider the scientific progress that could be realized from the analysis of bed materials at a  
275 particular site. With the goal of constraining Pleistocene GrIS history in mind, we consider four  
276 primary criteria.

277 First, the best sites should be robust monitors of past ice-sheet margin change. There  
278 could be regions, such as high-elevation terrain (e.g., in mountainous East Greenland) that meet  
279 the technical criteria but retain local ice cover during times of reduced ice-sheet configurations,  
280 complicating the link between the study site and broader GrIS change. There could also be sites  
281 that are part of the GrIS but are better conceived of as separate ice domes connected to the ice  
282 sheet via a saddle; these 'local' domes may persist longer than the adjacent ice sheet during  
283 interglacial periods as disconnected ice caps (e.g., Prudhoe Dome, Figure 5).



284           Second, to best capitalize on new measurements of cosmogenic nuclide signatures of  
285 past ice sheet changes (Spector et al., 2018; Keisling et al., 2022), sites should be sought that  
286 have persistent frozen-bedded conditions throughout glacial–interglacial cycles. These sites  
287 should favor preservation of cosmogenic nuclides at the ice–bed surface and reduce the  
288 likelihood of significant periods of time with subglacial erosion that removes the cosmogenic  
289 nuclide inventory. Identifying these sites could be based on a combination of selecting  
290 presently frozen bedded areas, favoring high-elevation locations or ice divide areas likely to be  
291 frozen bedded during past larger ice-sheet configurations, and evaluating paleo ice-sheet  
292 models to find ideal drilling locations.

293           Third, there may be some sites that are more sensitive monitors of reduced ice extent  
294 than others. For example, while some sites at 600 m ice thickness today may become ice free at  
295 under 5% reduction in ice-sheet mass, others may not become ice-free until a substantially  
296 greater reduction in mass. Using numerical ice-sheet models could greatly assist site selection  
297 and help to further explore sites that meet the technical requirements for their potential to  
298 constrain past ice sheet configurations (Keisling et al., 2022).

299           Fourth, some ice-sheet margin areas that include large, fast-flowing outlet glaciers with  
300 beds below sea level (e.g., near Jakobshavn Isbræ, Petermann Glacier, Northeast Greenland Ice  
301 Stream), could potentially ‘collapse’ at rates faster than other ice sheet margin areas. Thus,  
302 sites neighboring these regions, such as the Northeast Greenland Ice Stream, could not only  
303 serve as a binary signal of ice sheet presence/absence, but could help to elucidate the response  
304 of major outlet glaciers influenced by ice–ocean interactions to past climate forcing. Does the  
305 Northeast Greenland Ice Stream collapse during past warm times and exhibit proportionally  
306 more ice sheet recession than other ice-sheet sectors? Sites adjacent to the Northeast  
307 Greenland Ice Stream could help resolve this question.

308

#### 309 **4. Areas suitable for drilling using ASIG**

310           We synthesized the information discussed above to derive a map of candidate areas  
311 across the GrIS for drilling (Figure 3C). While only 3.4% of the GrIS bed is well suited for  
312 subglacial access for our purposes, there are several promising candidate sites: (1) Northwest



313 Greenland, specifically the metamorphic lithologies of the Ellesmere-Inglefield Province in  
314 Prudhoe Land-Inglefield Land; (2) Two regions in North Greenland: a small area around the  
315 head of Victoria Fjord that likely exposes metamorphic lithologies of the Victoria Province and  
316 an area adjacent to Mylius-Erichsen Land in eastern North Greenland that contains siliciclastic  
317 sedimentary units; (3) Dronning Louise Land in Northeast Greenland, where both crystalline  
318 and siliciclastic lithologies are present; and 4) central East Greenland, where the GrIS flows  
319 through alpine terrain of mixed lithology en route to the headwaters of the Scoresby Sund,  
320 Kong Oscar Fjord and Kejser Franz Joseph Fjord systems. There are additional small areas  
321 scattered around the periphery of the GrIS; however, most areas are in alpine-style, icefield-  
322 type settings, or lie in small areas between outlet glaciers.

323

#### 324 **4.1 Northwest Greenland: Prudhoe Land and Inglefield Land**

325 In Northwest Greenland, the ice sheet in Prudhoe Land and Inglefield Land has broad  
326 areas that meet the technical, safety and lithology criteria (Figures 3C and 5). Here, there are  
327 basement rocks consisting of Proterozoic metamorphic lithologies. Proportionally much of the  
328 region contains quartz-bearing metamorphic rocks (e.g., paragneiss), albeit with varying quartz  
329 content, and in some cases with bands of marble and other potentially non-quartz-bearing  
330 units (e.g., syenite, amphibolite; Henriksen et al., 2009). Further, the ice sheet has been  
331 surveyed extensively by NASA's Operation IceBridge and abundant radar data exist. The ice  
332 sheet margin adjacent to Inglefield Land, spanning between Hiawatha Crater and Prudhoe  
333 Dome, is roughly parabolic in profile and rather uniform in velocity, with surface speeds mostly  
334 ranging from 3–10 m yr<sup>-1</sup>. The topography of the ice sheet bed is low-relief, potentially making  
335 it difficult to identify small hills and swales where the substrate is less or more likely to host  
336 sediment. The landscape fronting the ice is largely bedrock, or bedrock overlain by surface  
337 blocks either frost-riven or slightly modified by former glaciation. In a few areas, alluvium or  
338 glacial deposits exist at the surface. Prudhoe Dome itself (Figure 5) has a thickness of ~500 m at  
339 a summit ridge that rests along a topographic high above a bed elevation of ~800 m asl. The  
340 velocities in the summit region of Prudhoe Dome range up to ~20 m yr<sup>-1</sup>. The Prudhoe Dome  
341 summit is a promising place to drill, with a high probability of encountering bedrock at the ice



342 sheet bed. However, upon deglaciation, the site may maintain local ice isolated from the inland  
343 ice, potentially fueled by snowfall due to its proximity to Baffin Bay.

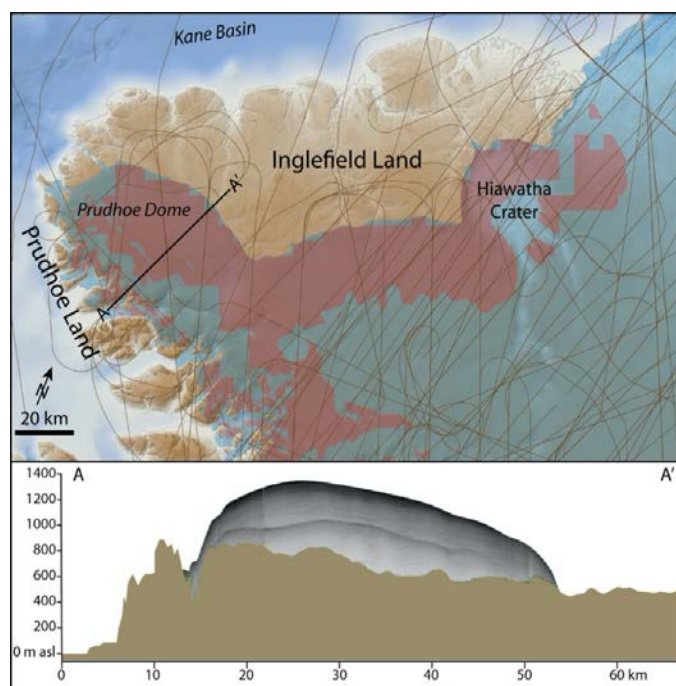


**Figure 5.** Top panel shows areas that meet drilling requirements (shown in red) in NW Greenland. The Greenland Ice Sheet is depicted in light blue, and NASA Operation Ice Bridge (OIB) flight lines are shown as thin brown lines. Bottom panel shows OIB radar of Prudhoe Dome along A-A', with topography, the ice-sheet bed and the ice-sheet surface from radar collected in 2017; the mid-ice-sheet reflector is the surface multiple. Basemap topography and bathymetry from Morlighem et al. (2017).

344

#### 345 **4.2 North Greenland: Victoria Fjord**

346 Most of North Greenland is dominated by sedimentary rocks of the lower Paleozoic  
347 Franklinian Basin not well suited for providing the hard, quartz-bearing lithologies that work  
348 best for in-situ cosmogenic nuclide analysis (Henriksen et al., 2009). At the head of Victoria  
349 Fjord (Figure 6A), however, Henriksen and Jepsen (1985) describe isolated outcrops of  
350 crystalline basement in otherwise non-quartz-bearing sedimentary-rock-dominated North  
351 Greenland. The crystalline rocks, mostly orthogneiss, comprise several nunataks in Victoria  
352 Fjord, and additionally crop out in the bottom of two valleys between C.H. Ostenfeld and Ryder  
353 glaciers (Figure 6B). The sedimentary formations consist of Neoproterozoic through Silurian  
354 lithologies composed of near-horizontally bedded shale, siltstone and abundant carbonate

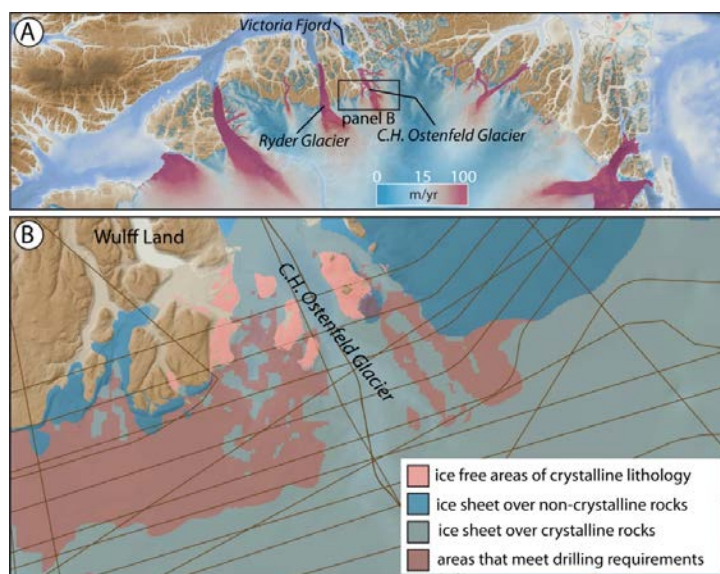
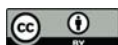


**Figure 6.** A. North Greenland showing ice sheet surface velocity; velocity from Greenland Ice Sheet velocity map from Sentinel-1, winter campaign 2019/2020 [version 1.3]; QGreenland v2.0. B. Areas that meet drilling requirements with a focus on bedrock lithology: bright blue are areas under the ice sheet with non-quartz bearing lithologies whereas the more muted blue colors depict our estimate of where there are quartz-bearing lithologies at the ice bed. Pink areas are quartz-bearing lithologies beyond the ice margin, and shown in muted red color are the areas that meet the drilling requirements. NASA Operation Ice Bridge (OIB) flight lines are shown as thin brown lines. Basemap topography and bathymetry from Morlighem et al. (2017).

355 units. The outcrop pattern is one of crystalline rocks exposed at lower elevations where the  
356 GrIS had eroded away the overlying sub-horizontal sedimentary rocks, or cap rocks. Overall, the  
357 outcrop of these quartz-bearing lithologies is promising for their existence at the ice-sheet bed  
358 south of the ice sheet margin. However, because there are topographic highs along the GrIS  
359 bed south of the margin, blindly drilling into areas that meet the other technical requirements  
360 could lead to encountering cap rocks. For this region, we perform an additional step to estimate  
361 where the bed south of the ice margin may be crystalline vs. sedimentary. To project the  
362 crystalline/cap rock contact southward under the ice sheet, we use the contact between  
363 crystalline rocks and the overlying cap rocks in exposed areas to perform a “3-point problem”  
364 an established method for determining the strike and dip of a plane based on geologic outcrop  
365 patterns. As observed by Henriksen and Jepsen (1985), the contact dips gently to the north, and  
366 the plane that we created in ArcGIS confirms this. Our estimation reveals crystalline rocks





367 outcropping in topographic low areas, and cap rocks outcropping in topographic high areas  
368 (Figure 6B). Our estimated contact is simplistic, as there may be folding and faulting that limit  
369 the accuracy of this extrapolation. However, this solution provides a straightforward estimate  
370 for where crystalline rocks may exist at the ice–bed interface near the head of Victoria Fjord.  
371 Using this information, along with Operation IceBridge flight lines and in combination with  
372 areas that meet the other technical and safety requirements, indicates promising areas to drill  
373 to the southwest of the onset zone of C.H. Ostenfeld Gletscher (Figure 6B).

374

#### 375 **4.3 North Greenland: Mylius-Erichsen Land**

376 In eastern North Greenland there is an ~100-km stretch of ice margin in Mylius-Erichsen  
377 Land (Figure 7) that lies over quartz-bearing sedimentary lithologies of the Proterozoic  
378 Independence Fjord Group (Henriksen et al., 2009). The rocks in this region contain near-  
379 horizontally bedded siltstones, sandstones, and quartzites intruded by Mesoproterozoic

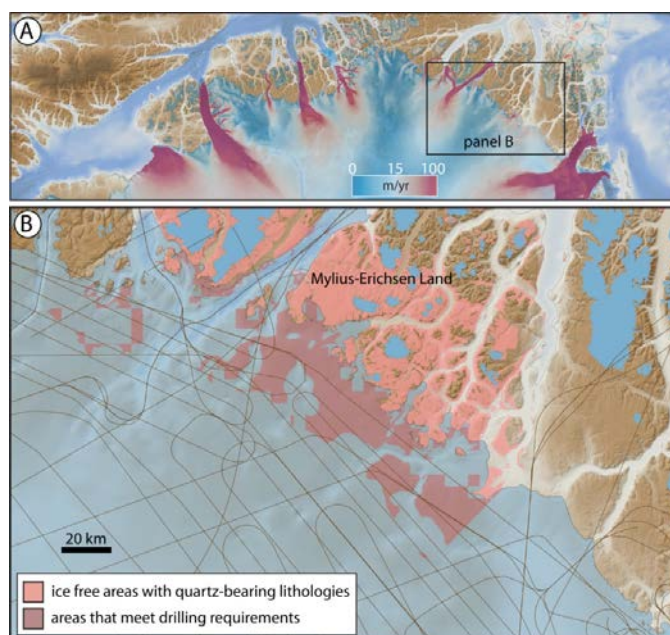
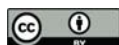


**Figure 7.** A. North Greenland showing ice sheet surface velocity; velocity from Greenland Ice Sheet velocity map from Sentinel-1, winter campaign 2019/2020 [version 1.3]; QGreenland v2.0. B. Mylius-Erichsen Land showing areas that meet drilling requirements, with pink areas representing quartz-bearing sedimentary formations (with mafic intrusives) beyond the ice margin. NASA Operation Ice Bridge (OIB) flight lines are shown as thin brown lines. Basemap topography and bathymetry from Morlighem et al. (2017).

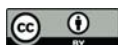


380 dolerite sills, dikes and stocks. Significant portions of the ice sheet in this region meet the  
381 technical and safety requirements for drilling, so the suitability for developing GfIS histories  
382 rests mostly on the likelihood of encountering preferred lithologies. The pattern on the geologic  
383 map and the unit description of the rock formations in the area indicate that the abundance of  
384 mafic intrusions mean that drilling has a reasonable chance of encountering non-quartz-bearing  
385 lithologies. The region has relatively sparse radar data that cross drilling-suitable areas  
386 compared to other parts of Greenland, narrowing the choices of drill sites that have tight  
387 constraints on ice thickness and bed shape.

388

#### 389 **4.4 Northeast Greenland: Dronning Louise Land**

390 The nunatak region of Dronning Louise Land, Northeast Greenland, contains broad areas  
391 that meet the technical requirements for subglacial drilling (Figure 8). The bedrock geology is  
392 part of the Caledonian fold belt and contains abundant structures that formed during the  
393 Caledonian Orogeny (Ordovician-Devonian) leading to the juxtaposition of crystalline and  
394 younger sedimentary rock formations in a complicated map pattern (Henriksen et al., 2009;  
395 Strachan et al., 2018). The broadest regions that meet our technical criteria and are most  
396 favorable for drilling lie on the western (inland) portion of the coastal mountain ranges. Here,  
397 nunataks exist 25-30 km west of the coastal mountains and provide information on the bedrock  
398 geology most relevant to potential drilling areas. The lithologies are similar to and have been  
399 correlated with the Independence Fjord Group found in Mylius-Erichsen Land. Specifically, the  
400 local unit that comprises inland nunataks (the Trekant Series) consists largely of quartzitic and  
401 feldspathic sandstone and conglomerate with intercalated siltstone and mudstone. Bedrock  
402 mapping in the nearby coastal mountains also reveals Mesoproterozoic dolerite intrusions.  
403 Sparse radar data limits potential drill sites with close constraints on ice thickness and bed  
404 shape. Yet, the region does have potential for tapping into quartz-bearing units and due to its  
405 proximity to the Northeast Greenland Ice Stream, sub-ice cosmogenic nuclide analyses from the  
406 area could yield important constraints on Northeast Greenland Ice Stream history. Finally, the  
407 possibility that high-elevation areas remain glaciated by local ice after inland ice recedes should  
408 not be ignored. Many of the sub-ice drilling targets are >1000 m asl, near twentieth century



409 snowline elevations. Thus, targeting lower-elevation parts of the sub-ice terrain could be  
410 advantageous given our goal to monitor GrIS history. The region has relatively sparse radar data  
411 coverage, suggesting that additional radar surveys over key areas would be useful for tightening  
412 constraints on ice thickness and bed topography over the frozen-bedded patches of Dronning  
413 Louise Land.

414

#### 415 4.5 East Greenland

416 A final place to highlight is central East Greenland, where – similar to Dronning Louise  
417 Land – the GrIS abuts and flows through alpine terrain. The western (inland) flank of these  
418 mountains has dozens of isolated areas that meet the technical requirements of drilling to the  
419 bed (Figure 9). Like the other areas throughout East and Northeast Greenland, the bedrock  
420 geology is highly variable. The headwaters of the Scoresby Sund, Kong Oscar Fjord and Kejser

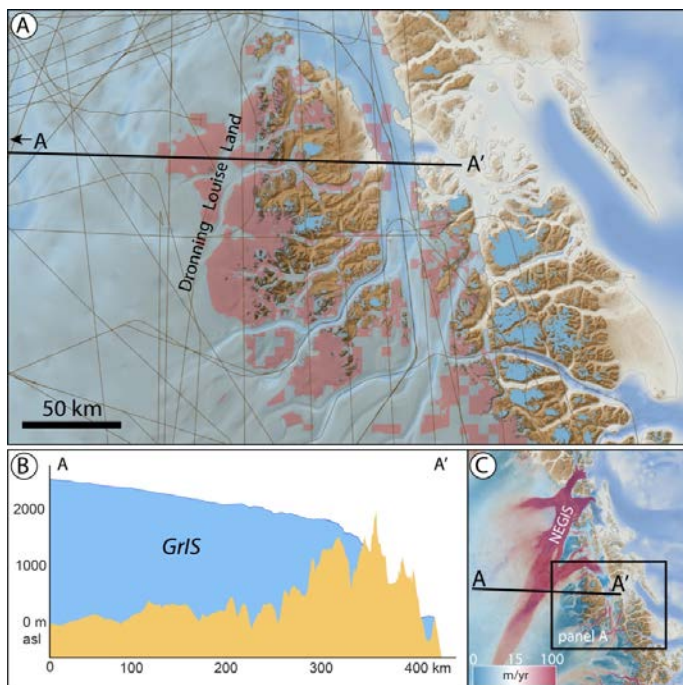
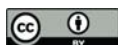


**Figure 8.** A. Dronning Louise Land showing areas that meet drill requirements; NASA Operation Ice Bridge (OIB) flight lines are shown as thin brown lines. B. Topographic profile of bed and GrIS surface from Bed Machine v3 (Morlighem et al., 2017); cross section line shown in panel C. C. NE Greenland with surface velocity showing NEGIS and location of panel A; velocity from Greenland Ice Sheet velocity map from Sentinel-1, winter campaign 2019/2020 [version 1.3]; QGreenland v2.0.. Basemap topography and bathymetry from Morlighem et al. (2017).



421 Franz Joseph Fjord systems have a complicated geology relating to the Caledonian Orogen,  
422 consisting of Paleoproterozoic crystalline metamorphic and sedimentary formations that are in  
423 turn slightly metamorphosed (Henriksson et al., 2009). In terms of finding quartz-bearing rocks  
424 most suitable for cosmogenic nuclide analysis, the region is heterogeneously made up of  
425 quartz-bearing (e.g., orthogneiss) and non-quartz-bearing formations (various fine-grained  
426 siliciclastic lithologies with occasional mafic intrusions). Inland nunataks provide knowledge of  
427 bedrock geology most proximal to potential drill locations and are largely composed of pelitic  
428 lithologies (e.g., metamorphosed mudstones). Looking closely at nunatak lithologies reveals  
429 some westernmost nunataks of orthogneiss composition, such as inland of J.L. Mowinckel Land  
430 (Figure 9), making the areas in this region that meet the technical requirement promising. A  
431 consideration with the potential drilling locations in central East Greenland, again, is the  
432 likelihood that they are deglaciated with the recession of inland ice, as opposed to retaining  
433 local ice cover. Airborne radar data are also sparse there, so care would be needed to select  
434 sites with the best constraints of ice thickness and bed shape.  
435

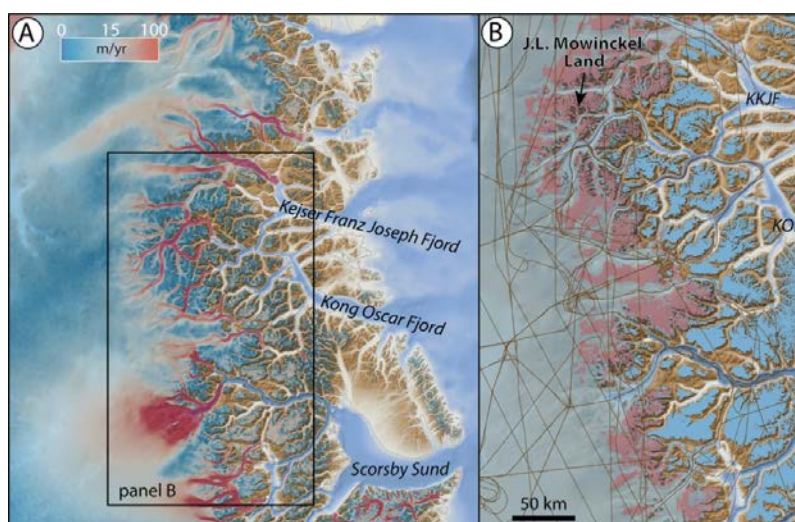
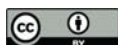


**Figure 9.** A. East Greenland showing GrIS flowing through alpine terrain; surface velocity highlights major outlets; velocity from Greenland Ice Sheet velocity map from Sentinel-1, winter campaign 2019/2020 [version 1.3]; QGreenland v2.0. B. Portion of East Greenland that includes the most areas that meet the technical requirements of drilling to the bed. Basemap topography and bathymetry from Morlighem et al. (2017).



436 **5. Conclusions**

437 Each of the two cases in Greenland in which cosmogenic nuclides have been analyzed in  
438 sub-ice material has led to significant insights into the history of the GrIS (Schaefer et al., 2016;  
439 Christ et al., 2020). Some of this new information – the time periods and duration of the  
440 Quaternary Period in which the GrIS was significantly reduced and/or largely absent – led to a  
441 reevaluation of the existing paradigm of GrIS expansion at the Quaternary boundary and  
442 general stability thereafter (Briner et al., 2017). This paradigm-shifting information from the  
443 GISP2 and Camp Century sites was based on archived material that was not collected  
444 specifically for sub-ice cosmogenic nuclide analysis. The purpose of this study is to identify  
445 potential targets for subglacial drilling *with* future cosmogenic nuclide analysis in mind. We find  
446 that only 3.4% of the GrIS is well suited for cosmogenic-nuclide analysis of bed materials using  
447 existing drills available from the US Ice Drilling Program and highlight five promising locations in  
448 northern and eastern Greenland. Future advances in drill capability, such as the ability to drill  
449 through thicker or wet-based ice, would significantly increase the area available for drilling  
450 (Figure 2).

451 In addition to obtaining drill cores of rock or sediment from the ice sheet bed, samples  
452 of other basal material would also benefit the research community. Basal ice is valuable for (1)  
453 measuring trace gasses to obtain basal ice age (Bender et al., 2010, Yau et al., 2016b), (2)  
454 detrital cosmogenic nuclide analysis of its mineral component (Bierman et al., 2014), and (3)  
455 ancient DNA and biomarkers in organic compounds (Willerslev et al., 2007). Boreholes  
456 themselves that are the product of drilling can be instrumented, resulting in direct  
457 measurements of basal heat flux values that would provide additional constraints on the basal  
458 thermal state of the GrIS (e.g., MacGregor et al., 2022; Colgan et al., 2021) and the history of  
459 the Iceland hotspot (e.g., Rogozhina et al., 2016). Finally, precise sampling at the ice-bed  
460 interface could lead to the discovery of ancient soils that plausibly exist in areas targeted for  
461 drilling that are frozen-bedded for long periods. Such samples may be useful for a variety of  
462 studies including ancient DNA, macrofossil, and biomarker analyses. Additionally, with proper  
463 precautions, the uppermost few millimeters of the bed can be preserved in light-free conditions



464 and used to measure for luminescence dating, providing an additional chronometer of past ice-  
465 sheet presence/absence (e.g., Christ et al., 2021).

466 In summary, we consider this study, and ideally drilling efforts taking place in one or  
467 more of these candidate sites, as only one of several next steps in the exploration of the GrIS  
468 bed. We recommend development of drills that can penetrate thicker ice and potentially ice  
469 where the bed is thawed. This could be done by modifying existing drill technology (e.g.,  
470 Timoney et al., 2020; Goodge et al., 2021) or require the development of entirely new drills.  
471 Expanding the area of the GrIS available for subglacial drilling would broaden the range of  
472 scientific questions that could be addressed regarding GrIS history and the range of possible  
473 targets. The application of cosmogenic nuclide analysis of subglacial materials could then move  
474 beyond constraining GrIS history during periods when it is only slightly smaller (~90%) than its  
475 present configuration to constraining times of significant reduction (~<10%). Additionally, there  
476 would be more resolving power for a fuller range of scientific questions, such as what shape the  
477 GrIS takes during past interglacials (Plach et al., 2018; Domingo et al., 2020), where ice  
478 dynamics may influence large-scale retreat (Aschwanden et al., 2019), or where there are  
479 packages of subglacial lake sediments (e.g., Keisling et al., 2020; Paxman et al., 2021) or unique  
480 geologic structures (Kjær et al., 2018; MacGregor et al., 2019). Evolving drilling techniques and  
481 analyses like this pave the way for targeted exploration of subglacial bed environments, a new  
482 frontier in ice sheet and sea level science.

483

#### 484 **Author contribution**

485 JB led the analysis and writing. CW led geographic-information-system computations. All  
486 authors contributed to discussions that resulted in the ideas and analysis presented in this  
487 manuscript, and all authors contributed to writing and presentation.

488

#### 489 **Acknowledgement**

490 This work was funded with NSF grant 1933938 (JPB) and 1933927 (NEY, JMS, BAK).

491

#### 492 **References**



493

494 Albert, M. R., Slawny, K. R., Boeckmann, G. V., Gibson, C. J., Johnson, J. A., Makinson, K., and Rix, J.: Recent  
495 innovations in drilling in ice, 2020.

496

497 Aschwanden, A., Fahnestock Mark, A., Truffer, M., Brinkerhoff Douglas, J., Hock, R., Khroulev, C., Mottram, R.,  
498 and Khan, S. A.: Contribution of the Greenland Ice Sheet to sea level over the next millennium, *Science*  
499 *Advances*, 5, eaav9396, 10.1126/sciadv.aav9396, 2019.

500

501 Balco, G.: Glacier Change and Paleoclimate Applications of Cosmogenic-Nuclide Exposure Dating, *Annual*  
502 *Review of Earth and Planetary Sciences*, 48, 21-48, 10.1146/annurev-earth-081619-052609, 2020.

503

504 Balter-Kennedy, A., Young, N. E., Briner, J. P., Graham, B. L., and Schaefer, J. M.: Centennial- and Orbital-Scale  
505 Erosion Beneath the Greenland Ice Sheet Near Jakobshavn Isbræ, *Journal of Geophysical Research: Earth*  
506 *Surface*, 126, e2021JF006429, <https://doi.org/10.1029/2021JF006429>, 2021.

507

508 Bender, M. L., Burgess, E., Alley, R. B., Barnett, B., and Clow, G. D.: On the nature of the dirty ice at the  
509 bottom of the GISP2 ice core, *Earth and Planetary Science Letters*, 299, 466-473,  
510 <https://doi.org/10.1016/j.epsl.2010.09.033>, 2010.

511

512 Bierman Paul, R., Corbett Lee, B., Graly Joseph, A., Neumann Thomas, A., Lini, A., Crosby Benjamin, T., and  
513 Rood Dylan, H.: Preservation of a Preglacial Landscape Under the Center of the Greenland Ice Sheet, *Science*,  
514 344, 402-405, 10.1126/science.1249047, 2014.

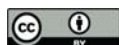
515

516 Bierman, P. R., Shakun, J. D., Corbett, L. B., Zimmerman, S. R., and Rood, D. H.: A persistent and dynamic East  
517 Greenland Ice Sheet over the past 7.5 million years, *Nature*, 540, 256-260, 10.1038/nature20147, 2016.

518

519 Briner, J. P., Cuzzone, J. K., Badgeley, J. A., Young, N. E., Steig, E. J., Morlighem, M., Schlegel, N.-J., Hakim, G.  
520 J., Schaefer, J. M., Johnson, J. V., Lesnek, A. J., Thomas, E. K., Allan, E., Bennike, O., Cluett, A. A., Csatho, B., de  
521 Vernal, A., Downs, J., Larour, E., and Nowicki, S.: Rate of mass loss from the Greenland Ice Sheet will exceed  
522 Holocene values this century, *Nature*, 586, 70-74, 10.1038/s41586-020-2742-6, 2020.

523

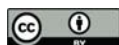


- 524 Briner, J. P., Lifton, N. A., Miller, G. H., Refsnider, K., Anderson, R., and Finkel, R.: Using in situ cosmogenic  
525  $^{10}\text{Be}$ ,  $^{14}\text{C}$ , and  $^{26}\text{Al}$  to decipher the history of polythermal ice sheets on Baffin Island, Arctic Canada,  
526 *Quaternary Geochronology*, 19, 4-13, <https://doi.org/10.1016/j.quageo.2012.11.005>, 2014.  
527
- 528 Briner, J. P., Miller, G. H., Davis, P. T., and Finkel, R. C.: Cosmogenic radionuclides from fiord landscapes  
529 support differential erosion by overriding ice sheets, *GSA Bulletin*, 118, 406-420, 10.1130/B25716.1, 2006.  
530
- 531 Briner, J. P., Stewart, H. A. M., Young, N. E., Philipps, W., and Losee, S.: Using proglacial-threshold lakes to  
532 constrain fluctuations of the Jakobshavn Isbræ ice margin, western Greenland, during the Holocene,  
533 *Quaternary Science Reviews*, 29, 3861-3874, <https://doi.org/10.1016/j.quascirev.2010.09.005>, 2010.  
534
- 535 Christ, A. J., Bierman, P. R., Knutz, P. C., Corbett, L. B., Fosdick, J. C., Thomas, E. K., Cowling, O. C., Hidy, A. J.,  
536 and Caffee, M. W.: The Northwestern Greenland Ice Sheet During The Early Pleistocene Was Similar To  
537 Today, *Geophysical Research Letters*, 47, e2019GL085176, <https://doi.org/10.1029/2019GL085176>, 2020.  
538
- 539 Christ Andrew, J., Bierman Paul, R., Schaefer Joerg, M., Dahl-Jensen, D., Steffensen Jørgen, P., Corbett Lee, B.,  
540 Peteet Dorothy, M., Thomas Elizabeth, K., Steig Eric, J., Rittenour Tammy, M., Tison, J.-L., Blard, P.-H.,  
541 Perdrial, N., Dethier David, P., Lini, A., Hidy Alan, J., Caffee Marc, W., and Southon, J.: A multimillion-year-old  
542 record of Greenland vegetation and glacial history preserved in sediment beneath 1.4 km of ice at Camp  
543 Century, *Proceedings of the National Academy of Sciences*, 118, e2021442118, 10.1073/pnas.2021442118,  
544 2021.  
545
- 546 Cluett Allison, A. and Thomas Elizabeth, K.: Summer warmth of the past six interglacials on Greenland,  
547 *Proceedings of the National Academy of Sciences*, 118, e2022916118, 10.1073/pnas.2022916118, 2021.  
548
- 549 Colgan, W., MacGregor, J. A., Mankoff, K. D., Haagensohn, R., Rajaram, H., Martos, Y. M., Morlighem, M.,  
550 Fahnestock, M. A., and Kjeldsen, K. K.: Topographic Correction of Geothermal Heat Flux in Greenland and  
551 Antarctica, *Journal of Geophysical Research: Earth Surface*, 126, e2020JF005598,  
552 <https://doi.org/10.1029/2020JF005598>, 2021.  
553
- 554 Dahl-Jensen, D., Albert, M. R., Aldahan, A., Azuma, N., Balslev-Clausen, D., Baumgartner, M., Berggren, A. M.,  
555 Bigler, M., Binder, T., Blunier, T., Bourgeois, J. C., Brook, E. J., Buchardt, S. L., Buizert, C., Capron, E.,  
556 Chappellaz, J., Chung, J., Clausen, H. B., Cvijanovic, I., Davies, S. M., Ditlevsen, P., Eicher, O., Fischer, H., Fisher,  
557 D. A., Fleet, L. G., Gfeller, G., Gkinis, V., Gogineni, S., Goto-Azuma, K., Grinsted, A., Gudlaugsdottir, H.,





558 Guillevic, M., Hansen, S. B., Hansson, M., Hirabayashi, M., Hong, S., Hur, S. D., Huybrechts, P., Hvidberg, C. S.,  
559 Iizuka, Y., Jenk, T., Johnsen, S. J., Jones, T. R., Jouzel, J., Karlsson, N. B., Kawamura, K., Keegan, K., Kettner, E.,  
560 Kipfstuhl, S., Kjær, H. A., Koutnik, M., Kuramoto, T., Köhler, P., Laepple, T., Landais, A., Langen, P. L., Larsen, L.  
561 B., Leuenberger, D., Leuenberger, M., Leuschen, C., Li, J., Lipenkov, V., Martinerie, P., Maselli, O. J., Masson-  
562 Delmotte, V., McConnell, J. R., Miller, H., Mini, O., Miyamoto, A., Montagnat-Rentier, M., Mulvaney, R.,  
563 Muscheler, R., Orsi, A. J., Paden, J., Pantón, C., Pattyn, F., Petit, J. R., Pol, K., Popp, T., Possnert, G., Prié, F.,  
564 Prokopiou, M., Quiquet, A., Rasmussen, S. O., Raynaud, D., Ren, J., Reutenauer, C., Ritz, C., Röckmann, T.,  
565 Rosen, J. L., Rubino, M., Rybak, O., Samyn, D., Sapart, C. J., Schilt, A., Schmidt, A. M. Z., Schwander, J.,  
566 Schüpbach, S., Seierstad, I., Severinghaus, J. P., Sheldon, S., Simonsen, S. B., Sjolte, J., Solgaard, A. M., Sowers,  
567 T., Sperlich, P., Steen-Larsen, H. C., Steffen, K., Steffensen, J. P., Steinhage, D., Stocker, T. F., Stowasser, C.,  
568 Sturevik, A. S., Sturges, W. T., Sveinbjörnsdóttir, A., Svensson, A., Tison, J. L., Uetake, J., Vallelonga, P., van de  
569 Wal, R. S. W., van der Wel, G., Vaughn, B. H., Vinther, B., Waddington, E., Wegner, A., Weikusat, I., White, J.  
570 W. C., Wilhelms, F., Winstrup, M., Witrant, E., Wolff, E. W., Xiao, C., Zheng, J., and members, N. c.: Eemian  
571 interglacial reconstructed from a Greenland folded ice core, *Nature*, 493, 489-494, [10.1038/nature11789](https://doi.org/10.1038/nature11789),  
572 2013.  
573  
574 Dawes, P. R.: The bedrock geology under the Inland Ice: the next major challenge for Greenland mapping,  
575 *GEUS Bulletin*, 17, 57-60, [10.34194/geusb.v17.5014](https://doi.org/10.34194/geusb.v17.5014), 2009.  
576  
577 de Vernal, A. and Hillaire-Marcel, C.: Natural Variability of Greenland Climate, Vegetation, and Ice Volume  
578 During the Past Million Years, *Science*, 320, 1622-1625, [10.1126/science.1153929](https://doi.org/10.1126/science.1153929), 2008.  
579  
580 DeConto, R. M., Pollard, D., Alley, R. B., Velicogna, I., Gasson, E., Gomez, N., Sadai, S., Condron, A., Gilford, D.  
581 M., Ashe, E. L., Kopp, R. E., Li, D., and Dutton, A.: The Paris Climate Agreement and future sea-level rise from  
582 Antarctica, *Nature*, 593, 83-89, [10.1038/s41586-021-03427-0](https://doi.org/10.1038/s41586-021-03427-0), 2021.  
583  
584 Domingo, D., Malmierca-Vallet, I., Sime, L., Voss, J., and Capron, E.: Using Ice Cores and Gaussian Process  
585 Emulation to Recover Changes in the Greenland Ice Sheet During the Last Interglacial, *Journal of Geophysical*  
586 *Research: Earth Surface*, 125, e2019JF005237, <https://doi.org/10.1029/2019JF005237>, 2020.  
587  
588 Dyer, B., Austermann, J., D'Andrea William, J., Creel Roger, C., Sandstrom Michael, R., Cashman, M., Rovere,  
589 A., and Raymo Maureen, E.: Sea-level trends across The Bahamas constrain peak last interglacial ice melt,  
590 *Proceedings of the National Academy of Sciences*, 118, e2026839118, [10.1073/pnas.2026839118](https://doi.org/10.1073/pnas.2026839118), 2021.  
591



- 592 Goelzer, H., Huybrechts, P., Loutre, M. F., and Fichet, T.: Last Interglacial climate and sea-level evolution  
593 from a coupled ice sheet–climate model, *Clim. Past*, 12, 2195–2213, 10.5194/cp-12-2195-2016, 2016.  
594
- 595 Goelzer, H., Nowicki, S., Payne, A., Larour, E., Seroussi, H., Lipscomb, W. H., Gregory, J., Abe-Ouchi, A.,  
596 Shepherd, A., Simon, E., Agosta, C., Alexander, P., Aschwanden, A., Barthel, A., Calov, R., Chambers, C., Choi,  
597 Y., Cuzzone, J., Dumas, C., Edwards, T., Felikson, D., Fettweis, X., Golledge, N. R., Greve, R., Humbert, A.,  
598 Huybrechts, P., Le clec'h, S., Lee, V., Leguy, G., Little, C., Lowry, D. P., Morlighem, M., Nias, I., Quiquet, A.,  
599 Rückamp, M., Schlegel, N. J., Slater, D. A., Smith, R. S., Straneo, F., Tarasov, L., van de Wal, R., and van den  
600 Broeke, M.: The future sea-level contribution of the Greenland ice sheet: a multi-model ensemble study of  
601 ISMIP6, *The Cryosphere*, 14, 3071–3096, 10.5194/tc-14-3071-2020, 2020.  
602
- 603 Goodge, J. W. and Severinghaus, J. P.: Rapid Access Ice Drill: a new tool for exploration of the deep Antarctic  
604 ice sheets and subglacial geology, *Journal of Glaciology*, 62, 1049–1064, 10.1017/jog.2016.97, 2016.  
605 Granger, D. E., Lifton, N. A., and Willenbring, J. K.: A cosmic trip: 25 years of cosmogenic nuclides in geology,  
606 *GSA Bulletin*, 125, 1379–1402, 10.1130/B30774.1, 2013.  
607
- 608 Hatfield, R. G., Reyes, A. V., Stoner, J. S., Carlson, A. E., Beard, B. L., Winsor, K., and Welke, B.: Interglacial  
609 responses of the southern Greenland ice sheet over the last 430,000 years determined using particle-size  
610 specific magnetic and isotopic tracers, *Earth and Planetary Science Letters*, 454, 225–236,  
611 <https://doi.org/10.1016/j.epsl.2016.09.014>, 2016.  
612
- 613 Henriksen, N., Higgins, A. K., Kalsbeek, F., and Pulvertaft, T. C. R.: Greenland from Archaean to Quaternary.  
614 Descriptive text to the 1995 Geological map of Greenland, 1:2 500 000. 2nd edition, *GEUS Bulletin*, 18, 1–126,  
615 10.34194/geusb.v18.4993, 2009.  
616
- 617 Henriksen, N. and Jepsen, H. F.: Precambrian crystalline basement at the head of Victoria Fjord, North  
618 Greenland, *Rapport Grønlands Geologiske Undersøgelse*, 126, 11–16, 10.34194/rapggu.v126.7907, 1985.  
619 Jordan, T. M., Williams, C. N., Schroeder, D. M., Martos, Y. M., Cooper, M. A., Siegert, M. J., Paden, J. D.,  
620 Huybrechts, P., and Bamber, J. L.: A constraint upon the basal water distribution and thermal state of the  
621 Greenland Ice Sheet from radar bed echoes, *The Cryosphere*, 12, 2831–2854, 10.5194/tc-12-2831-2018, 2018.  
622
- 623 Joughin, I., Das, S. B., Flowers, G. E., Behn, M. D., Alley, R. B., King, M. A., Smith, B. E., Bamber, J. L., van den  
624 Broeke, M. R., and van Angelen, J. H.: Influence of ice-sheet geometry and supraglacial lakes on seasonal ice-  
625 flow variability, *The Cryosphere*, 7, 1185–1192, 10.5194/tc-7-1185-2013, 2013.



626

627 Keisling, B. A., Nielsen, L. T., Hvidberg, C. S., Nuterman, R., and DeConto, R. M.: Pliocene–Pleistocene

628 megafloods as a mechanism for Greenlandic megacanyon formation, *Geology*, 48, 737-741,

629 10.1130/G47253.1, 2020.

630

631 Keisling, B.A., Schaefer, J.M., DeConto, R.M., Briner, J.P., Young, N.E., Walcott, C., Winckler, G., Balter-

632 Kennedy, A., Anandakrishnan, S.: Greenland ice sheet vulnerability under diverse climatic warming scenarios,

633 Earth ArXiv, doi.org/10.31223/X5Q05T, 2022.

634

635 Knutz, P. C., Newton, A. M. W., Hopper, J. R., Huuse, M., Gregersen, U., Sheldon, E., and Dybkjær, K.: Eleven

636 phases of Greenland Ice Sheet shelf-edge advance over the past 2.7 million years, *Nature Geoscience*, 12,

637 361-368, 10.1038/s41561-019-0340-8, 2019.

638

639 Kuhl, T., Gibson, C., Johnson, J., Boeckmann, G., Moravec, E., and Slawny, K.: Agile Sub-Ice Geological (ASIG)

640 Drill development and Pirrit Hills field project, *Annals of Glaciology*, 62, 53-66, 10.1017/aog.2020.59, 2021.

641

642 Kulessa, B., Hubbard Alun, L., Booth Adam, D., Bougamont, M., Dow Christine, F., Doyle Samuel, H.,

643 Christoffersen, P., Lindbäck, K., Pettersson, R., Fitzpatrick Andrew, A. W., and Jones Glenn, A.: Seismic

644 evidence for complex sedimentary control of Greenland Ice Sheet flow, *Science Advances*, 3, e1603071,

645 10.1126/sciadv.1603071, 2017.

646

647 Li, J., Paden, J., Leuschen, C., Rodriguez-Morales, F., Hale, R. D., Arnold, E. J., Crowe, R., Gomez-Garcia, D., and

648 Gogineni, P.: High-Altitude Radar Measurements of Ice Thickness Over the Antarctic and Greenland Ice

649 Sheets as a Part of Operation IceBridge, *IEEE Transactions on Geoscience and Remote Sensing*, 51, 742-754,

650 10.1109/TGRS.2012.2203822, 2013.

651

652 MacGregor, J. A., Bottke Jr, W. F., Fahnestock, M. A., Harbeck, J. P., Kjær, K. H., Paden, J. D., Stillman, D. E.,

653 and Studinger, M.: A Possible Second Large Subglacial Impact Crater in Northwest Greenland, *Geophysical*

654 *Research Letters*, 46, 1496-1504, <https://doi.org/10.1029/2018GL078126>, 2019.

655

656 MacGregor, J. A., Chu, W., Colgan, W. T., Fahnestock, M. A., Felikson, D., Karlsson, N. B., Nowicki, S. M. J., and

657 Studinger, M.: GBaTSv2: A revised synthesis of the likely basal thermal state of the Greenland Ice Sheet, *The*

658 *Cryosphere Discuss.*, 2022, 1-25, 10.5194/tc-2022-40, 2022.

659



- 660 MacGregor, J. A., Fahnestock, M. A., Colgan, W. T., Larsen, N. K., Kjeldsen, K. K., and Welker, J. M.: The age of  
661 surface-exposed ice along the northern margin of the Greenland Ice Sheet, *Journal of Glaciology*, 66, 667-684,  
662 10.1017/jog.2020.62, 2020.
- 663
- 664 McNabb, R. W., Hock, R., O'Neel, S., Rasmussen, L. A., Ahn, Y., Braun, M., Conway, H., Herreid, S., Joughin, I.,  
665 Pfeiffer, W. T., Smith, B. E., and Truffer, M.: Using surface velocities to calculate ice thickness and bed  
666 topography: a case study at Columbia Glacier, Alaska, USA, *Journal of Glaciology*, 58, 1151-1164,  
667 10.3189/2012JoG11J249, 2012.
- 668
- 669 Morlighem, M., Rignot, E., Mouginot, J., Seroussi, H., and Larour, E.: Deeply incised submarine glacial valleys  
670 beneath the Greenland ice sheet, *Nature Geoscience*, 7, 418-422, 10.1038/ngeo2167, 2014.
- 671
- 672 Morlighem, M., Rignot, E., Seroussi, H., Larour, E., Ben Dhia, H., and Aubry, D.: A mass conservation approach  
673 for mapping glacier ice thickness, *Geophysical Research Letters*, 38, <https://doi.org/10.1029/2011GL048659>,  
674 2011.
- 675
- 676 Morlighem, M., Williams, C. N., Rignot, E., An, L., Arndt, J. E., Bamber, J. L., Catania, G., Chauché, N.,  
677 Dowdeswell, J. A., Dorschel, B., Fenty, I., Hogan, K., Howat, I., Hubbard, A., Jakobsson, M., Jordan, T. M.,  
678 Kjeldsen, K. K., Millan, R., Mayer, L., Mouginot, J., Noël, B. P. Y., O'Cofaigh, C., Palmer, S., Rysgaard, S.,  
679 Seroussi, H., Siegert, M. J., Slabon, P., Straneo, F., van den Broeke, M. R., Weinrebe, W., Wood, M., and  
680 Zinglensen, K. B.: BedMachine v3: Complete Bed Topography and Ocean Bathymetry Mapping of Greenland  
681 From Multibeam Echo Sounding Combined With Mass Conservation, *Geophysical Research Letters*, 44,  
682 11,051-011,061, <https://doi.org/10.1002/2017GL074954>, 2017.
- 683
- 684 Nishiizumi, K., Finkel, R. C., Ponganis, K. V., Graf, T., Kohl, C. P., and Marti, K.: In situ produced cosmogenic  
685 nuclides in GISP2 rock core from Greenland summit, *Eos*, 77, F428, 1996.
- 686
- 687 Paxman, G. J. G., Austermann, J., and Tinto, K. J.: A fault-bounded palaeo-lake basin preserved beneath the  
688 Greenland Ice Sheet, *Earth and Planetary Science Letters*, 553, 116647,  
689 <https://doi.org/10.1016/j.epsl.2020.116647>, 2021.
- 690
- 691 Pedersen, M., Weng, W. L., Keulen, N., and Kokfelt, T. F.: A new seamless digital 1:500 000 scale geological  
692 map of Greenland, *GEUS Bulletin*, 28, 65-68, 10.34194/geusb.v28.4727, 2013.
- 693



- 694 Plach, A., Nisancioglu, K. H., Le clec'h, S., Born, A., Langebroek, P. M., Guo, C., Imhof, M., and Stocker, T. F.:  
695 Eemian Greenland SMB strongly sensitive to model choice, *Clim. Past*, 14, 1463-1485, 10.5194/cp-14-1463-  
696 2018, 2018.
- 697
- 698 Poinar, K. and Andrews, L. C.: Challenges in predicting Greenland supraglacial lake drainages at the regional  
699 scale, *The Cryosphere*, 15, 1455-1483, 10.5194/tc-15-1455-2021, 2021.
- 700
- 701 Reyes, A. V., Carlson, A. E., Beard, B. L., Hatfield, R. G., Stoner, J. S., Winsor, K., Welke, B., and Ullman, D. J.:  
702 South Greenland ice-sheet collapse during Marine Isotope Stage 11, *Nature*, 510, 525-528,  
703 10.1038/nature13456, 2014.
- 704
- 705 Robinson, A., Alvarez-Solas, J., Calov, R., Ganopolski, A., and Montoya, M.: MIS-11 duration key to  
706 disappearance of the Greenland ice sheet, *Nature Communications*, 8, 16008, 10.1038/ncomms16008, 2017.
- 707
- 708 Rogozhina, I., Petrunin, A. G., Vaughan, A. P. M., Steinberger, B., Johnson, J. V., Kaban, M. K., Calov, R.,  
709 Rickers, F., Thomas, M., and Koulakov, I.: Melting at the base of the Greenland ice sheet explained by Iceland  
710 hotspot history, *Nature Geoscience*, 9, 366-369, 10.1038/ngeo2689, 2016.
- 711
- 712 Scambos, T. A., Bell, R. E., Alley, R. B., Anandkrishnan, S., Bromwich, D. H., Brunt, K., Christianson, K., Creyts,  
713 T., Das, S. B., DeConto, R., Dutrieux, P., Fricker, H. A., Holland, D., MacGregor, J., Medley, B., Nicolas, J. P.,  
714 Pollard, D., Siegfried, M. R., Smith, A. M., Steig, E. J., Trusel, L. D., Vaughan, D. G., and Yager, P. L.: How much,  
715 how fast?: A science review and outlook for research on the instability of Antarctica's Thwaites Glacier in the  
716 21st century, *Global and Planetary Change*, 153, 16-34, <https://doi.org/10.1016/j.gloplacha.2017.04.008>,  
717 2017.
- 718
- 719 Schaefer, J. M., Finkel, R. C., Balco, G., Alley, R. B., Caffee, M. W., Briner, J. P., Young, N. E., Gow, A. J., and  
720 Schwartz, R.: Greenland was nearly ice-free for extended periods during the Pleistocene, *Nature*, 540, 252-  
721 255, 10.1038/nature20146, 2016.
- 722
- 723 Shepherd, A., Ivins, E., Rignot, E., Smith, B., van den Broeke, M., Velicogna, I., Whitehouse, P., Briggs, K.,  
724 Joughin, I., Krinner, G., Nowicki, S., Payne, T., Scambos, T., Schlegel, N., A. G., Agosta, C., Ahlstrøm, A.,  
725 Babonis, G., Barletta, V., Blazquez, A., Bonin, J., Csatho, B., Cullather, R., Felikson, D., Fettweis, X., Forsberg,  
726 R., Gallee, H., Gardner, A., Gilbert, L., Groh, A., Gunter, B., Hanna, E., Harig, C., Helm, V., Horvath, A.,  
727 Horwath, M., Khan, S., Kjeldsen, K. K., Konrad, H., Langen, P., Lecavalier, B., Loomis, B., Luthcke, S., McMillan,



728 M., Melini, D., Mernild, S., Mohajerani, Y., Moore, P., Mouginit, J., Moyano, G., Muir, A., Nagler, T., Nield, G.,  
729 Nilsson, J., Noel, B., Ootosaka, I., Pattle, M. E., Peltier, W. R., Pie, N., Rietbroek, R., Rott, H., Sandberg-  
730 Sørensen, L., Sasgen, I., Save, H., Scheuchl, B., Schrama, E., Schröder, L., Seo, K.-W., Simonsen, S., Slater, T.,  
731 Spada, G., Sutterley, T., Talpe, M., Tarasov, L., van de Berg, W. J., van der Wal, W., van Wessem, M.,  
732 Vishwakarma, B. D., Wiese, D., Wouters, B., and The, I. t.: Mass balance of the Antarctic Ice Sheet from 1992  
733 to 2017, *Nature*, 558, 219-222, 10.1038/s41586-018-0179-y, 2018.  
734  
735 Shepherd, A., Ivins, E., Rignot, E., Smith, B., van den Broeke, M., Velicogna, I., Whitehouse, P., Briggs, K.,  
736 Joughin, I., Krinner, G., Nowicki, S., Payne, T., Scambos, T., Schlegel, N., A. G., Agosta, C., Ahlstrøm, A.,  
737 Babonis, G., Barletta, V. R., Bjørk, A. A., Blazquez, A., Bonin, J., Colgan, W., Csatho, B., Cullather, R., Engdahl,  
738 M. E., Felikson, D., Fettweis, X., Forsberg, R., Hogg, A. E., Gallee, H., Gardner, A., Gilbert, L., Gourmelen, N.,  
739 Groh, A., Gunter, B., Hanna, E., Harig, C., Helm, V., Horvath, A., Horwath, M., Khan, S., Kjeldsen, K. K., Konrad,  
740 H., Langen, P. L., Lecavalier, B., Loomis, B., Luthcke, S., McMillan, M., Melini, D., Mernild, S., Mohajerani, Y.,  
741 Moore, P., Mottram, R., Mouginit, J., Moyano, G., Muir, A., Nagler, T., Nield, G., Nilsson, J., Noël, B., Ootosaka,  
742 I., Pattle, M. E., Peltier, W. R., Pie, N., Rietbroek, R., Rott, H., Sandberg Sørensen, L., Sasgen, I., Save, H.,  
743 Scheuchl, B., Schrama, E., Schröder, L., Seo, K.-W., Simonsen, S. B., Slater, T., Spada, G., Sutterley, T., Talpe,  
744 M., Tarasov, L., van de Berg, W. J., van der Wal, W., van Wessem, M., Vishwakarma, B. D., Wiese, D., Wilton,  
745 D., Wagner, T., Wouters, B., Wuite, J., and The, I. T.: Mass balance of the Greenland Ice Sheet from 1992 to  
746 2018, *Nature*, 579, 233-239, 10.1038/s41586-019-1855-2, 2020.  
747  
748 Sommers, A. N., Otto-Bliesner, B. L., Lipscomb, W. H., Lofverstrom, M., Shafer, S. L., Bartlein, P. J., Brady, E. C.,  
749 Kluzek, E., Leguy, G., Thayer-Calder, K., and Tomas, R. A.: Retreat and Regrowth of the Greenland Ice Sheet  
750 During the Last Interglacial as Simulated by the CESM2-CISM2 Coupled Climate–Ice Sheet Model,  
751 *Paleoceanography and Paleoclimatology*, 36, e2021PA004272, <https://doi.org/10.1029/2021PA004272>, 2021.  
752  
753 Spector, P., Stone, J., Cowdery, S. G., Hall, B., Conway, H., and Bromley, G.: Rapid early-Holocene deglaciation  
754 in the Ross Sea, Antarctica, *Geophysical Research Letters*, 44, 7817-7825,  
755 <https://doi.org/10.1002/2017GL074216>, 2017.  
756  
757 Spector, P., Stone, J., Pollard, D., Hillebrand, T., Lewis, C., and Gombiner, J.: West Antarctic sites for subglacial  
758 drilling to test for past ice-sheet collapse, *The Cryosphere*, 12, 2741-2757, 10.5194/tc-12-2741-2018, 2018.  
759  
760 Sugden, D. E.: Glacial Erosion by the Laurentide Ice Sheet, *Journal of Glaciology*, 20, 367-391,  
761 10.3189/S0022143000013915, 1978.



762

763 Timoney, R., Worrall, K., Firstbrook, D., Harkness, P., Rix, J., Ashurst, D., Mulvaney, R., and Bentley, M. J.: A  
764 low resource subglacial bedrock sampler: The percussive rapid access isotope drill (P-RAID), *Cold Regions*  
765 *Science and Technology*, 177, 103113, <https://doi.org/10.1016/j.coldregions.2020.103113>, 2020.

766

767 Willerslev, E., Cappellini, E., Boomsma, W., Nielsen, R., Hebsgaard Martin, B., Brand Tina, B., Hofreiter, M.,  
768 Bunce, M., Poinar Hendrik, N., Dahl-Jensen, D., Johnsen, S., Steffensen Jørgen, P., Bennike, O., Schwenninger,  
769 J.-L., Nathan, R., Armitage, S., de Hoog, C.-J., Alfimov, V., Christl, M., Beer, J., Muscheler, R., Barker, J., Sharp,  
770 M., Penkman Kirsty, E. H., Haile, J., Taberlet, P., Gilbert, M. T. P., Casoli, A., Campani, E., and Collins Matthew,  
771 J.: Ancient Biomolecules from Deep Ice Cores Reveal a Forested Southern Greenland, *Science*, 317, 111-114,  
772 [10.1126/science.1141758](https://doi.org/10.1126/science.1141758), 2007.

773

774 Yau, A. M., Bender, M. L., Blunier, T., and Jouzel, J.: Setting a chronology for the basal ice at Dye-3 and GRIP:  
775 Implications for the long-term stability of the Greenland Ice Sheet, *Earth and Planetary Science Letters*, 451,  
776 1-9, <https://doi.org/10.1016/j.epsl.2016.06.053>, 2016.

777

778 Yau Audrey, M., Bender Michael, L., Robinson, A., and Brook Edward, J.: Reconstructing the last interglacial at  
779 Summit, Greenland: Insights from GISP2, *Proceedings of the National Academy of Sciences*, 113, 9710-9715,  
780 [10.1073/pnas.1524766113](https://doi.org/10.1073/pnas.1524766113), 2016.

781

782 Young, N. E., Lesnek, A. J., Cuzzone, J. K., Briner, J. P., Badgeley, J. A., Balter-Kennedy, A., Graham, B. L.,  
783 Cluett, A., Lamp, J. L., Schwartz, R., Tuna, T., Bard, E., Caffee, M. W., Zimmerman, S. R. H., and Schaefer, J. M.:  
784 In situ cosmogenic  $^{10}\text{Be}$ – $^{14}\text{C}$ – $^{26}\text{Al}$  measurements from recently deglaciated bedrock as a new tool to  
785 decipher changes in Greenland Ice Sheet size, *Climate of the Past*, 17, 419-450, [http://dx.doi.org/10.5194/cp-](http://dx.doi.org/10.5194/cp-17-419-2021)  
786 [17-419-2021](https://doi.org/10.5194/cp-17-419-2021), 2021.